4

Constructing wavelet frames and orthogonal wavelet bases on the sphere

Daniela Roşca[a] and Jean-Pierre Antoine[b]
[a]*Department of Mathematics, Technical University of Cluj-Napoca*
RO-400020 Cluj-Napoca, Romania
Daniela.Rosca@math.utcluj.ro
[b]*Institut de Physique Théorique, Université catholique de Louvain*
B-1348 Louvain-la-Neuve, Belgium
Jean-Pierre.Antoine@uclouvain.be

1. Introduction

A classical problem is to analyse a signal (function) by decomposing it into suitable building blocks, then approximate it by truncating the expansion. Well-known examples are Fourier transform and its localized version, the Short Time Fourier transform (sometimes called the Gabor transform), and the wavelet transform. In the best case, the elementary blocks form a basis in the space of signals, with the pleasant consequence that the expansion coefficients are uniquely defined. Unfortunately, this is not always possible and often one has to resort to frames. In image processing, in particular, two-dimensional wavelets are by now a standard tool in image processing, under the two concurrent approaches, the Discrete Wavelet Transform (DWT), based on the concept of multiresolution analysis, and the Continuous Wavelet Transform (CWT). While the former usually leads to wavelet bases, the CWT has to be discretized for numerical implementation and produces in general only frames.

Nowadays, many situations yield data on *spherical* surfaces. For instance, in Earth and Space sciences (geography, geodesy, meteorology, astronomy, cosmology, etc), in crystallography (texture analysis of crystals), in medicine (some organs are regarded as sphere-like surfaces), or in computer graphics (modelling of closed surfaces as the graph of a function defined on the sphere). So one needs a suitable analysis tool for such data. In the spherical case, the Fourier transform amounts to an expansion in spherical harmonics, whose support is the whole sphere. Fourier analysis on the sphere is thus global and cumbersome. Therefore many different methods have been proposed to replace it with some sort of wavelet analysis.

In addition, some data may live on more complicated manifolds, such as a *two-sheeted hyperboloid*, in cosmology for instance (an open expanding model of the universe). In optics also, in the catadioptric image processing, where a sensor overlooks a mirror with the shape of a hyperboloid or a *paraboloid*. Another example is a closed *sphere-like surface*, that is, a surface obtained from a sphere by a smooth deformation. Thus it would be useful to have a wavelet transform available on such manifolds as well.

In this chapter, we will review the various aspects of the wavelet transform on the two-sphere, both continuous and discrete, with some emphasis on the construction of bases and frames.

We will also quickly indicate generalizations to other curved manifolds. Besides the original papers, partial reviews of some of this material may be found in (Antoine & Vandergheynst, 2007; Antoine & Roşca, 2008). The present chapter is an elaboration of the paper (Roşca & Antoine, 2008).

2. The CWT on the two-sphere

2.1 Heuristics

We consider first the extension of the CWT to the two sphere $\mathbb{S}^2 = \{\mathbf{x} \in \mathbb{R}^3,\ \|\mathbf{x}\| = 1\}$. A complete solution was obtained in (Antoine & Vandergheynst, 1999; Antoine et al., 2002) by a group-theoretical method (which actually works in any dimension (Antoine & Vandergheynst, 1998)). As it is well-known in the planar case, the design of a CWT on a given manifold X starts by identifying the operations one wants to perform on the finite energy signals living on X, that is, functions in $L^2(X, dv)$, where v is a suitable measure on X. Next one realizes these operations by unitary operators on $L^2(X, dv)$ and one looks for a possible group-theoretical derivation.

In the case of the two-sphere $\mathbb{S}^2$, the required transformations are of two types: (i) *motions*, which are realized by rotations $\varrho \in \mathrm{SO}(3)$, and (ii) *dilations* of some sort by a scale factor $a \in \mathbb{R}_+^*$. The problem is how to define properly the dilation *on* the sphere $\mathbb{S}^2$. The solution proposed in (Antoine & Vandergheynst, 1999; Antoine et al., 2002) consists in lifting onto the sphere, by inverse *stereographic projection*, the usual radial dilation in the tangent plane at the South Pole. More precisely, one proceeds in three steps: Project a point $A \in \mathbb{S}^2$ onto the point B in the tangent plane, perform the usual 2-D dilation $B \mapsto B_a$ by a factor a, and project back to $A_a \in \mathbb{S}^2$. The map $A \mapsto A_a$ is the *stereographic dilation.*

Now, the Hilbert space of spherical signals is $L^2(\mathbb{S}^2, d\mu)$, where $d\mu = \sin\theta\, d\theta\, d\varphi$, $\theta \in [0, \pi]$ is the colatitude angle, $\varphi \in [0, 2\pi)$ the longitude angle, $\omega = (\theta, \varphi) \in \mathbb{S}^2$. In that space, the desired operations are realized by the following unitary operators:

$$\text{. rotation } R_\varrho \ :\ (R_\varrho f)(\omega) = f(\varrho^{-1}\omega),\ \varrho \in \mathrm{SO}(3), \tag{1}$$

$$\text{. dilation } D_a \ :\ (D_a f)(\omega) = \lambda(a,\theta)^{1/2} f(\omega_{1/a}),\ a \in \mathbb{R}_+^*. \tag{2}$$

In relation (2), $\omega_a := (\theta_a, \varphi)$, θ_a is defined by $\cot\frac{\theta_a}{2} = a\cot\frac{\theta}{2}$ for $a > 0$ and the normalization factor (Radon-Nikodym derivative, cocycle) , given as

$$\lambda(a,\theta)^{1/2} := 2a\left[(a^2-1)\cos\theta + (a^2+1)\right]^{-1}, \tag{3}$$

is needed for compensating the noninvariance under dilation of the natural measure $d\mu(\omega)$ on $\mathbb{S}^2$. Thus, starting from a function $\psi \in L^2(\mathbb{S}^2)$, we consider the whole family it generates, namely, $\{\psi_{\varrho,a} := R_\varrho D_a \psi,\ \varrho \in \mathrm{SO}(3),\ a > 0\}$.

By analogy with the plane case, the spherical wavelet transform of a function $f \in L^2(\mathbb{S}^2)$, with respect to the wavelet ψ, will be defined as

$$W_\psi f(\varrho, a) := \langle \psi_{\varrho,a} | f \rangle. \tag{4}$$

The question, of course, is to determine which functions ψ can qualify as wavelets, that is, to determine the wavelet admissibility condition. Apart from an educated guess, the natural way to find the answer is through a group-theoretical analysis, mimicking the familiar one of planar 2-D wavelets.

2.2 The group-theoretical or coherent state approach

As a matter of fact, this spherical CWT was obtained in (Antoine & Vandergheynst, 1999) by the group-theoretical approach familiar in the planar 2-D case. The point is to embed the rotations from SO(3) and the dilations into the Lorentz group $\mathrm{SO}_o(3,1)$, the argument being that this group is the *conformal* group both of the sphere $\mathbb{S}^2$ and of the tangent plane $\mathbb{R}^2$. The embedding results from the so-called *Iwasawa decomposition*:

$$\mathrm{SO}_o(3,1) = \mathrm{SO}(3) \cdot A \cdot N,$$

where $A \sim \mathrm{SO}_o(1,1) \sim \mathbb{R} \sim \mathbb{R}_*^+$ (boosts in the z-direction) and $N \sim \mathbb{C}$.
Then it turns out that the Lorentz group $\mathrm{SO}_o(3,1)$ has a transitive action on the sphere $\mathbb{S}^2$. In particular, a boost from A corresponds to a stereographic dilation. Now $\mathrm{SO}_o(3,1)$ has a natural unitary representation U in $L^2(\mathbb{S}^2, d\mu)$, namely,

$$[U(g)f](\omega) = \lambda(g,\omega)^{1/2} f\left(g^{-1}\omega\right), \text{ for } g \in \mathrm{SO}_o(3,1),\ f \in L^2(\mathbb{S}^2, d\mu), \tag{5}$$

where $\lambda(g,\omega) \equiv \lambda(a,\theta)$ is the Radon-Nikodym derivative (3).
Thus the parameter space of the spherical CWT is the quotient

$$X = \mathrm{SO}_o(3,1)/N \sim \mathrm{SO}(3) \cdot A,$$

which is *not* a group. Therefore, in order to apply the general formalism, we must introduce a *section* $\sigma : X \to \mathrm{SO}_o(3,1)$ and consider the reduced representation $U(\sigma(\varrho,a))$. Choosing the natural (Iwasawa) section $\sigma(\varrho,a) = \varrho\, a,\ \varrho \in \mathrm{SO}(3),\ a \in A$, we obtain

$$U(\sigma(\varrho,a)) = U(\varrho\, a) = U(\varrho)U(a) = R_\varrho\, D_a, \tag{6}$$

exactly as before, in (1)-(2).
The following three propositions show that the representation (5) has all the properties that are required to generate a useful CWT. First of all, it is square integrable on the quotient manifold $X = \mathrm{SO}_o(3,1)/N \simeq \mathrm{SO}(3) \cdot \mathbb{R}_*^+$. For simplicity, we shall identify these two isomorphic manifolds.

Proposition 2.1. *The UIR* (5) *is square integrable on X modulo the section σ, that is, there exist nonzero (admissible) vectors $\psi \in L^2(\mathbb{S}^2, d\mu)$ such that*

$$\int_0^\infty \frac{da}{a^3} \int_{\mathrm{SO}(3)} d\varrho\, |\langle U(\sigma(\varrho,a))\psi|\phi\rangle|^2 := \langle \phi | A_\psi \phi\rangle < \infty, \text{ for all } \phi \in L^2(\mathbb{S}^2, d\mu)\,. \tag{7}$$

Here $d\varrho$ is the left invariant (Haar) measure on SO(3).
The resolution operator *(also called* frame operator*) A_ψ is diagonal in Fourier space (i.e., it is a Fourier multiplier):*

$$\widehat{A_\psi f}(l,m) = G_\psi(l)\widehat{f}(l,m), \tag{8}$$

where

$$G_\psi(l) = \frac{8\pi^2}{2l+1} \sum_{|m|\leqslant l} \int_0^\infty \frac{da}{a^3} |\widehat{\psi}_a(l,m)|^2, \qquad \text{for all } l \in \mathbb{N}, \tag{9}$$

and $\widehat{\psi}_a(l,m) = \langle Y_l^m | \psi_a\rangle$, where Y_l^m is a spherical harmonic and $\psi_a := D_a\psi$.

Next, we have an exact admissibility condition on the wavelets (this condition was also derived by Holschneider (1996)).

Proposition 2.2. *An admissible wavelet is a function $\psi \in L^2(\mathbb{S}^2, d\mu)$ for which there exists a positive constant $c < \infty$ such that $G_\psi(l) \leqslant c$, for all $l \in \mathbb{N}$. Equivalently, the function $\psi \in L^2(\mathbb{S}^2, d\mu)$ is an admissible wavelet if and only if the resolution operator A_ψ is bounded and invertible.*

As in the plane case (Antoine et al., 2004), there is also a weaker admissibility condition on ψ:

$$\int_{\mathbb{S}^2} \frac{\psi(\theta, \varphi)}{1 - \cos\theta}\, d\mu(\omega) = 0. \tag{10}$$

Here too, this condition is only necessary in general, but it becomes sufficient under mild regularity conditions on ψ. This is clearly similar to the "zero mean" condition of wavelets on the line or the plane. As in the flat case, it implies that the spherical CWT acts as a *local filter*, in the sense that it selects the components of a signal that are similar to ψ, which is assumed to be well localized.
Finally, our spherical wavelets generate continuous frames. Indeed:

Proposition 2.3. *For any admissible wavelet ψ such that $\int_0^{2\pi} d\varphi\ \psi(\theta, \varphi) \neq 0$, the family $\{\psi_{a,\varrho} := R_\varrho\, D_a \psi : a > 0, \varrho \in \mathrm{SO}(3)\}$ is a continuous frame, that is, there exist two constants $\mathsf{m} > 0$ and $\mathsf{M} < \infty$ such that*

$$\mathsf{m}\, \|\phi\|^2 \leqslant \int_0^\infty \frac{da}{a^3} \int_{\mathrm{SO}(3)} d\varrho\, |\langle \psi_{a,\varrho} | \phi \rangle|^2 \leqslant \mathsf{M}\, \|\phi\|^2, \ \textit{for all}\ \ \phi \in L^2(\mathbb{S}^2, d\mu), \tag{11}$$

or, equivalently, there exist two positive constants $d > 0$ and $c < \infty$ such that

$$d \leqslant G_\psi(l) \leqslant c, \ \ \textit{for all}\ \ l \in \mathbb{N}$$

(in other words, the operators A_ψ and A_ψ^{-1} are both bounded).

Note that the condition $\int_0^{2\pi} d\varphi\ \psi(\theta, \varphi) \not\equiv 0$ is automatically satisfied for any nonzero axisymmetric (zonal) wavelet. The frame so obtained is not tight, unless $G_\psi(l) = \text{const}$. For an axisymmetric wavelet, $\widehat{\psi}_a(l, m) \equiv \widehat{\psi}_a(l)$ is independent of m, hence tightness would require that $G_\psi(l) = 8\pi^2 \int_0^\infty a^{-3} da\ |\widehat{\psi}_a(l)|^2 = \text{const}$, which seems difficult to obtain.
With all the ingredients thus available, we may now define the spherical CWT as in (4), namely,

Definition 2.4. *Given the admissible wavelet ψ, the* spherical CWT *of a function $f \in L^2(\mathbb{S}^2, d\mu)$ with respect to ψ is defined as*

$$W_\psi f(\varrho, a) := \langle \psi_{\varrho,a} | f \rangle = \int_{\mathbb{S}^2} \overline{[R_\varrho D_a \psi](\omega)}\, f(\omega)\, d\mu(\omega). \tag{12}$$

As in the planar case, this spherical CWT may be inverted and one gets the following *reconstruction formula*. For $f \in L^2(\mathbb{S}^2)$ and ψ an admissible wavelet such that $\int_0^{2\pi} \psi(\theta, \varphi)\, d\varphi \neq 0$, one has

$$f(\omega) = \int_{\mathbb{R}_+^*} \int_{SO(3)} W_\psi f(\varrho, a) [A_\psi^{-1} R_\varrho D_a \psi](\omega)\, a^{-3}\, da\, d\varrho.$$

In addition, the spherical CWT has two important properties:
(1) It has a correct *Euclidean limit*. By this we mean that, if we construct the transform on a sphere of radius R and then let $R \to \infty$, the spherical CWT tends to the usual planar 2-D

CWT on the tangent plane at the South Pole. We refer to (Antoine & Vandergheynst, 1999) for mathematical details.
(2) Unlike the usual 2-D CWT, which is fully covariant with respect to translations, rotations and dilations, the spherical CWT is only partially covariant. It is covariant under motions on $\mathbb{S}^2$: for any $\varrho_o \in \mathrm{SO}(3)$, the transform of the rotated signal $f(\varrho_o^{-1}\omega)$ is the function $W_\psi f(\varrho_o^{-1}\varrho, a)$. But it is *not* covariant under dilations. Indeed the wavelet transform of the dilated signal $(D_{a_o} f)(\omega) = \lambda(a_o, \theta)^{1/2} f(\omega_{1/a_o})$ is $\langle U(g)\psi | f\rangle$, with $g = a_o^{-1}\varrho a$, and the latter, while a well-defined element of $\mathrm{SO}_o(3,1)$, is *not* of the form $\sigma(\varrho', a')$. This reflects the fact that the parameter space X of the spherical CWT is not a group, but only a homogeneous space.
A byproduct of this analysis is a complete equivalence between the spherical CWT and the usual planar CWT in the tangent plane, in the sense that the stereographic projection induces a unitary map $\pi : L^2(\mathbb{S}^2) \to L^2(\mathbb{R}^2)$. This fact allows one to lift any plane wavelet, including directional ones, onto the sphere by inverse stereographic projection. The same technique will be used in Section 3.3 below for lifting the discrete WT onto the sphere and thus generating orthogonal wavelet bases on it.
The advantages of this method are that it is easy to implement (the wavelet ψ is given explicitly), it leaves a large freedom in choosing the mother wavelet ψ, it allows the use of directional wavelets, it preserves smoothness and it gives no distortion around poles, since all points of $\mathbb{S}^2$ are equivalent under the action of the operator R_ϱ. However, it is computationally intensive. As for the disadvantages, the method yields only frames, not bases, as we will see in the next section.
Although this spherical CWT was originally obtained by a group-theoretical method, this mathematically sophisticated approach may be short-circuited if one remarks that it is uniquely determined by the geometry, in the sense that it suffices to impose *conformal* behavior of the relevant maps. More precisely, the stereographic projection is the unique conformal diffeomorphism from the sphere to its tangent plane at the South Pole. Similarly, the stereographic dilation (2) is the unique longitude-preserving dilation on the sphere that is conformal (Wiaux et al., 2005). Thus one gets the formula (12) directly, without the group-theoretical calculation.
There is an alternative that also leads to a half-continuous wavelet representation on $\mathbb{S}^2$. It consists in using the so-called *harmonic* dilation instead of the stereographic one. This dilation acts on the Fourier coefficients of a function f, that is, the numbers $\widehat{f}_{\ell,m} := \langle Y_\ell^m | f\rangle_{\mathbb{S}^2}$, where $\{Y_\ell^m, \ell \in \mathbb{N}, m = -\ell, \ldots, \ell\}$ is the orthonormal basis of spherical harmonics in $L^2(\mathbb{S}^2)$. The dilation d_a is defined by the relation

$$\widehat{(d_a f)}_{\ell,m} := f_{a\ell,m}, \ a > 0.$$

This technique, originally due to Holschneider (1996) and Freeden & Windheuser (1997), has recently been revived in the applications to astrophysics (Wiaux et al., 2008). However, although this definition leads to a well-defined, uniquely invertible wavelet representation, with steerable wavelets and full rotation invariance, there is no proof so far that it yields a frame. Hence one may question the stability of the reconstruction process, since it is the lower frame bound that guarantees it.

2.3 Spherical frames

The spherical CWT (12) may be discretized and one obtains frames, either half-continuous (only the scale variable a is discretized) or fully discrete (Antoine et al., 2002; Bogdanova et al.,

2005). To be more precise, one gets generalized frames, called *weighted frames* and *controlled frames*, respectively. They are defined as follows (Jacques, 2004; Bogdanova et al., 2005; Balazs et al., 2009).
Let $\{\phi_n : n \in \mathcal{I}\}$ be a countable family of vectors in a (separable) Hilbert space $\mathfrak{H}$ (the index set $\mathcal{I}$ may be finite or infinite). Then, the family $\{\phi_n\}$ is a *weighted frame* in $\mathfrak{H}$ if there are positive weights w_n and two constants $\mathsf{m} > 0$ and $\mathsf{M} < \infty$ such that

$$\mathsf{m}\,\|f\|^2 \leqslant \sum_{n\in\mathcal{I}} w_n\,|\langle\phi_n|f\rangle|^2 \leqslant \mathsf{M}\,\|f\|^2, \text{ for all } f \in \mathfrak{H}. \tag{13}$$

The family $\{\phi_n\}$ is a *controlled frame* in $\mathfrak{H}$ if there is a positive bounded operator C, with bounded inverse, such that

$$\mathsf{m}\,\|f\|^2 \leqslant \sum_{n\in\mathcal{I}} \langle\phi_n|f\rangle\,\langle f|C\phi_n\rangle \leqslant \mathsf{M}\,\|f\|^2, \text{ for all } f \in \mathfrak{H}. \tag{14}$$

Clearly this reduces to standard frames for $w_n = \text{const}$ and $C = I$, respectively.
These two notions are in fact mathematically equivalent to the classical notion of frame, namely, a family of vectors $\{\phi_n\}$ is a weighted frame, resp. a controlled frame, if and only if it is a frame in the standard sense (with different frame bounds, of course) (Balazs et al., 2009). However, this is not true numerically, the convergence properties of the respective frame expansions may be quite different (Antoine et al., 2004; Bogdanova et al., 2005). And, indeed, the new notions were introduced precisely for improving the convergence of the reconstruction process.
Following Bogdanova et al. (2005), we first build a half-continuous spherical frame, by discretizing the scale variable only, while keeping continuous the position variable on the sphere. We choose the half-continuous grid $\Lambda = \{(\omega, a_j) : \omega \in \mathbb{S}^2, j \in \mathbb{Z}, a_j > a_{j+1}\}$, where $\mathcal{A} = \{a_j : j \in \mathbb{Z}\}$ is an arbitrary decreasing sequence of scales, and $\nu_j := (a_j - a_{j+1})/a_j^3$ are weights that mimic the natural (Haar) measure da/a^3. Then a tight frame might be obtained, as shown in following proposition.

Proposition 2.5. *Let $\mathcal{A} = \{a_j : j \in \mathbb{Z}\}$ be a decreasing sequence of scales. If ψ is an axisymmetric wavelet for which there exist two constants $\mathsf{m}, \mathsf{M} \in \mathbb{R}_+^*$ such that*

$$\mathsf{m} \leqslant g_\psi(l) \leqslant \mathsf{M}, \text{ for all } l \in \mathbb{N}, \tag{15}$$

where

$$g_\psi(l) = \frac{4\pi}{2l+1} \sum_{j\in\mathbb{Z}} \nu_j\,|\widehat{\psi}_{a_j}(l,0)|^2,$$

then any function $f \in L^2(\mathbb{S}^2, d\mu)$ may be reconstructed from the corresponding family of spherical wavelets, as

$$f(\omega) = \sum_{j\in\mathbb{Z}} \nu_j \int_{\mathbb{S}^2} d\mu(\omega')\, W_\psi f(\omega', a_j)\, \left[\ell_\psi^{-1} R_{[\omega']} D_{a_j}\psi\right](\omega'), \tag{16}$$

where ℓ_ψ is the (discretized) resolution operator defined by $\widehat{\ell_\psi^{-1}h}(l,m) = g_\psi(l)^{-1}\,h(l,m)$.

Note that the resolution operator ℓ_ψ is simply the discretized version of the continuous resolution operator A_ψ. Clearly (16) may be interpreted as a (weighted) tight frame controlled by the operator ℓ_ψ^{-1}.

Next, still following Bogdanova et al. (2005), one designs a fully discrete spherical frame by discretizing all the variables. The scale variable is discretized as before. As for the positions, we choose an equiangular grid $\mathcal{G}_j$ indexed by the scale level:

$$\mathcal{G}_j = \{\omega_{jpq} = (\theta_{jp}, \varphi_{jq}) \in \mathbb{S}^2 : \theta_{jp} = \tfrac{(2p+1)\pi}{4B_j}, \varphi_{jq} = \tfrac{q\pi}{B_j}\}, \tag{17}$$

for $p, q \in \mathcal{N}_j := \{n \in \mathbb{N} : n < 2B_j\}$ and some range of bandwidths $\mathcal{B} = \{B_j \in 2\mathbb{N} : j \in \mathbb{Z}\}$. Note that, in (17), the values $\{\theta_{jp}\}$ constitute a pseudo-spectral grid, with nodes on the zeros of a Chebyshev polynomial of degree $2B_j$. Their virtue is the existence of an *exact* quadrature rule (Driscoll & Healy, 1994), namely,

$$\int_{\mathbb{S}^2} d\mu(\omega) f(\omega) = \sum_{p,q \in \mathcal{N}_j} w_{jp}\, f(\omega_{jpq}), \tag{18}$$

with certain (explicit) weights $w_{jp} > 0$ and for every band-limited function $f \in L^2(\mathbb{S}^2, d\mu)$ of bandwidth B_j (i.e., $\widehat{f}(l,m) = 0$ for all $l \geqslant B_j$). Thus the complete discretization grid is $\Lambda(\mathcal{A}, \mathcal{B}) = \{(a_j, \omega_{jpq}) : j \in \mathbb{Z},\ p, q \in \mathcal{N}_j\}$.
For this choice of discretization grid, one obtains a discrete *weighted, nontight frame, controlled by the operator* A_ψ^{-1}, namely, $\{\psi_{jpq} = R_{[\omega_{jpq}]} D_{a_j} \psi : j \in \mathbb{Z},\ p, q \in \mathcal{N}_j\}$ (Bogdanova et al., 2005):

$$\mathsf{m}\, \|f\|^2 \leqslant \sum_{j \in \mathbb{Z}} \sum_{p,q \in \mathcal{N}_j} \nu_j w_{jp}\, W_\psi f(\omega_{jpq}, a_j)\, \overline{\widetilde{W}_\psi f(\omega_{jpq}, a_j)} \leqslant \mathsf{M}\, \|f\|^2, \tag{19}$$

where $\nu_j = (a_j - a_{j+1})/a_j^3$ are the same positive weights as in Proposition 2.5 and

$$\widetilde{W}_\psi f(\varrho, a) := \langle \widetilde{\psi}_{a,\varrho} | f \rangle = \langle A_\psi^{-1} R_\varrho D_a \psi | f \rangle. \tag{20}$$

A sufficient condition for (19) to hold may be given, but it is very complicated, involving the determinant of an ∞-dimensional matrix, unless f is band-limited. As usual, when the frame bounds are close enough, approximate reconstruction formulas may be used. The convergence of the process may still be improved by combining the reconstruction with a conjugate gradient algorithm.
As a matter of fact, no discretization scheme leading to a wavelet *basis* is known and, in practice, the method applies to band-limited functions only. This entails high *redundancy* and thus a higher computing cost, which is not suitable for large data sets. There is also the problem of finding an appropriate discretization grid which leads to good frames. Some of them, e.g. the equi-angular grid $\Lambda(\mathcal{A}, \mathcal{B})$ described above, yield exact quadrature rules for the integration of band-limited signals on $\mathbb{S}^2$, but other ones (typically, the familiar HEALPix) are only approximate. This is actually a general feature: when discretizing a CWT, it is not easy to prove that a given discretization leads to a frame, even less to a good frame or a tight frame.
For all those reasons, one would prefer to try and build directly a DWT on the sphere.

3. The DWT on the sphere

3.1 General requirements

Many authors have designed methods for constructing discrete spherical wavelets. All of them have advantages and drawbacks. These may be characterized in terms of several properties which are desirable for *any* efficient wavelet analysis, planar or spherical (a thorough discussion of this topic may be found in Antoine & Roşca (2008)).

· *Basis:* The redundancy of frames leads to nonunique expansions. Moreover, the existing constructions of spherical frames are sometimes computationally heavy and often applicable only to band-limited functions. Thus, in some applications, genuine bases are preferable.
· *Orthogonality:* This method leads to orthogonal reconstruction matrices, whose inversion is trivial. Thus, orthogonal bases are good for compression, but this is not always sufficient: sparsity of reconstruction matrices is still needed in the case of large data sets.
· *Local support:* This is crucial when working with large data sets, since it yields sparse matrices in the implementation of the algorithms. Also, it prevents spreading of "tails" during approximation.[1]
· *Continuity, smoothness:* These properties are always desirable in approximation, but not easily achieved.

3.2 Some known methods

Let us quote a few of those methods, with focus on the properties just mentioned, without being exhaustive. A more comprehensive review, with all references to original papers, may be found in (Antoine & Roşca, 2008).

(1) The spherical DWT using spherical harmonics

Various constructions of discrete spherical wavelets using spherical harmonics may be found in the literature, leading to frames or bases. The advantages of this method is that it produces no distortion (since no pole has a privileged role) and that it preserves smoothness of the wavelets. However, the wavelets so obtained have in general a localized support, but not a local one, i.e., it covers the whole sphere. Since this implies full reconstruction matrices, the result is not suitable for large amount of data. Examples are the works of Potts et al. (1996) or Freeden & Schreiner (1997).

(2) The spherical DWT via polar coordinates

The polar coordinate map $\rho : I = [0, \pi] \times [0, 2\pi) \to \mathbb{S}^2$ has the familiar form

$$\rho : (\theta, \varphi) \mapsto (\cos\varphi \sin\theta, \sin\varphi \sin\theta, \cos\theta) .$$

A problem here is *continuity*. Indeed a continuous function f defined on I remains continuous after mapping it onto $\mathbb{S}^2$ if and only if $f(\theta, 0) = f(\theta, 2\pi)$, for all $\theta \in [0, \pi]$, and there exists two constants P_N, P_S such that $f(0, \varphi) = P_N$ and $f(\pi, \varphi) = P_S$, for all $\varphi \in [0, 2\pi)$. Unfortunately, these continuity conditions are not easily satisfied by wavelets on intervals.
The obvious advantage of this approach is that many data sets are given in polar coordinates and thus one does not need to perform additional interpolation when implementing. However, there are disadvantages. First, no known construction gives both continuity and local support. Next, there are distortions around the poles: ρ maps the whole segment $\{(0, \varphi),\ \varphi \in [0, 2\pi)\}$ onto the North Pole, and the whole segment $\{(\pi, \varphi),\ \varphi \in [0, 2\pi)\}$ onto the South Pole. Representative examples are papers by Dahlke et al. (1995) or Weinreich (2001).

(3) The spherical DWT via radial projection from a convex polyhedron

Let $\mathbb{S}^2$ be the unit sphere centered in 0 and let Γ be a convex polyhedron, containing 0 in its interior and with triangular faces (if some faces are non-triangular, one simply triangularizes

[1] A wavelet has *local support* if it vanishes identically outside a small region. It is *localized* if it is negligible outside a small region, so that it may have (small, but nonzero) "tails" there. Since these tails may spread in the process of approximation of data and spoil their good localization properties, local support is definitely preferred (see the example in (Roşca & Antoine, 2009)).

them). The idea of the method, due to one of us (Roşca, 2005; 2007a;b), is to obtain wavelets on $\mathbb{S}^2$ first by moving planar wavelets to wavelets defined on the faces of Γ and then projecting these radially onto $\mathbb{S}^2$. This proceeds as follows. Let $\Omega = \partial\Gamma$ denote the boundary of Γ and let $p : \Omega \to \mathbb{S}^2$ denote the radial projection from the origin:

$$p(x,y,z) = \rho \cdot (x,y,z), \quad \text{where } \rho := \rho(x,y,z) = 1/\sqrt{x^2+y^2+z^2}.$$

Let $\mathcal{T}$ denote the set of triangular faces of Γ and consider the following weighted scalar product on $L^2(\mathbb{S}^2)$:

$$\langle F|G\rangle_\Gamma = \sum_{T\in\mathcal{T}} \int_{p(T)} F(\zeta)\, G(\zeta)\, w_T(\zeta)\, d\mu(\zeta), \quad \zeta = (\zeta_1,\zeta_2,\zeta_3) \in \mathbb{S}^2,\ F, G \in L^2(\mathbb{S}^2). \tag{21}$$

Here $w_T(\zeta_1,\zeta_2,\zeta_3) = 2d_T^2\,|a_T\zeta_1 + b_T\zeta_2 + c_T\zeta_3|^{-3}$, with a_T, b_T, c_T, d_T the coefficients of $x, y, z, 1$, respectively, in the determinant

$$\begin{vmatrix} x & y & z & 1 \\ x_1 & y_1 & z_1 & 1 \\ x_2 & y_2 & z_2 & 1 \\ x_3 & y_3 & z_3 & 1 \end{vmatrix} = a_T x + b_T y + c_T z + d_T 1,$$

where (x_i, y_i, z_i), $i = 1, 2, 3$, are the vertices of the planar triangle $T \in \mathcal{T}$. Then one proves that the norm $\|\cdot\|_\Gamma := \langle\cdot|\cdot\rangle_\Gamma^{1/2}$ is equivalent to the usual norm in $L^2(\mathbb{S}^2)$, i.e., there exist constants $\mathsf{m}_\Gamma > 0$, $\mathsf{M}_\Gamma < \infty$ such that

$$\mathsf{m}_\Gamma \|f\|_\Gamma \leqslant \|f\|_2 \leqslant \mathsf{M}_\Gamma \|f\|_\Gamma\,, \ \forall\, f \in L^2(\mathbb{S}^2).$$

Explicit expressions for optimal bounds m_Γ and M_Γ are given in (Roşca, 2009).
The resulting wavelets are orthogonal with respect to the weighted scalar product (21) on $L^2(\mathbb{S}^2)$. This method offers many advantages: no distortion around the poles, possible construction of continuous and locally supported stable wavelet bases, local support of the wavelets (leading to sparse matrices), easy implementation, possible extension to sphere-like surfaces (Roşca, 2006). As a disadvantage, we may note the lack of smoothness of the wavelets.

(4) Needlets

A new class of discrete spherical wavelets, called *needlets*, has been introduced recently (Narcowich et al., 2006a;b; Baldi et al., 2009). These functions, which are actually special spherical harmonics kernels, are derived by combining three ideas, namely, a Littlewood-Paley decomposition, a suitable distribution of (finitely many) points on the sphere, called *centers*, and an exact quadrature rule. The dilation takes place in the space of spherical harmonics, effectively in Fourier space, i.e., it is a harmonic dilation as described at the end of Section 2.2. The upshot is a new class of tight frames on the sphere. The frame functions are both compactly supported in the frequency domain (i.e., band-limited in l) and almost exponentially localized around each center. When combined with a new statistical method, they offer a powerful tool for analysing CMB (WMAP) data, e.g. for analysing the cross-correlation between the latter and galaxy counts from sky surveys (Pietrobon et al., 2006; Marinucci et al., 2008). They have also found nice applications in statistics (Baldi et al., 2008; 2009).
As a matter of fact, no construction so far has led to wavelet bases on the sphere which are *simultaneously* continuous (or smoother), orthogonal and locally supported, although any two of these three conditions may be met at the same time. This suggests to try another approach.

3.3 Lifting the DWT from the plane to the sphere

The method we propose consists in lifting wavelets from the tangent plane to the sphere by inverse stereographic projection (Roşca & Antoine, 2009). It yields simultaneously smoothness, orthogonality, local support, vanishing moments. The disadvantage is that it gives distortions around a pole. In addition, it is not suitable for the whole sphere $\mathbb{S}^2$, but only for data "away" from that pole. However, the latter can be taken anywhere on the sphere, for instance, in a region where no data is given. To give an example, European climatologists routinely put the North Pole of their spherical grid in the middle of the Pacific Ocean. Therefore, this is in fact a minor inconvenient in practice.

Our sphere is

$$\mathbb{S}^2 = \{\boldsymbol{\zeta} = (\zeta_1, \zeta_2, \zeta_3) \in \mathbb{R}^3,\ \zeta_1^2 + \zeta_2^2 + (\zeta_3 - 1)^2 = 1\},$$

where we have used the parametrization $\zeta_1 = \cos\varphi \sin\theta, \zeta_2 = \sin\varphi \sin\theta, \zeta_3 = 1 + \cos\theta$, for $\theta \in (0, \pi], \varphi \in [0, 2\pi)$. The pointed sphere is $\dot{\mathbb{S}}^2 = \mathbb{S}^2 \setminus \{(0, 0, 2)\}$.

Let now $\mathsf{p} : \dot{\mathbb{S}}^2 \to \mathbb{R}^2$ be the stereographic projection from the North Pole $N(0, 0, 2)$ onto the tangent plane $\zeta_3 = 0$ at the South Pole. The area elements $d\mathbf{x}$ of $\mathbb{R}^2$ and $\mu(\boldsymbol{\zeta})$ of $\dot{\mathbb{S}}^2$ are related by $d\mathbf{x} = \nu(\boldsymbol{\zeta})^2\, d\mu(\boldsymbol{\zeta})$, where the weight factor $\nu : \dot{\mathbb{S}}^2 \to \mathbb{R}$ is defined as

$$\nu(\boldsymbol{\zeta}) = \frac{2}{2 - \zeta_3} = \frac{2}{1 - \cos\theta},\ \boldsymbol{\zeta} = (\zeta_1, \zeta_2, \zeta_3) \equiv (\theta, \varphi) \in \dot{\mathbb{S}}^2.$$

Notice that $L^2(\dot{\mathbb{S}}^2) := L^2(\dot{\mathbb{S}}^2, d\mu(\boldsymbol{\zeta})) = L^2(\mathbb{S}^2)$, since the set $\{N\}$ is of measure zero. As mentioned in Section 2, the stereographic projection p induces a unitary map $\pi : L^2(\dot{\mathbb{S}}^2) \to L^2(\mathbb{R}^2)$, with inverse $\pi^{-1} : L^2(\mathbb{R}^2) \to L^2(\dot{\mathbb{S}}^2)$ given by $\pi^{-1}(F) = \nu \cdot (F \circ \mathsf{p}),\ \forall\, F \in L^2(\mathbb{R}^2)$. As a consequence, we have

$$\langle F | G \rangle_{L^2(\mathbb{R}^2)} = \langle \nu \cdot (F \circ \mathsf{p}) | \nu \cdot (G \circ \mathsf{p}) \rangle_{L^2(\dot{\mathbb{S}}^2)},\ \forall\, F, G \in L^2(\mathbb{R}^2). \tag{22}$$

This equality allows us to construct orthogonal bases on $L^2(\dot{\mathbb{S}}^2)$ starting from orthogonal bases in $L^2(\mathbb{R}^2)$. More precisely, we will use the fact that, if the functions $F, G \in L^2(\mathbb{R}^2)$ are orthogonal, then the functions $F^s = \nu \cdot (F \circ \mathsf{p})$ and $G^s = \nu \cdot (G \circ \mathsf{p})$ will be orthogonal in $L^2(\dot{\mathbb{S}}^2)$. Thus, the construction of multiresolution analysis (MRA) and wavelet bases in $L^2(\dot{\mathbb{S}}^2)$ is based on the equality (22).

The starting point is a MRA in $L^2(\mathbb{R}^2)$ (for a thorough analysis of MRAs in 1-D and in 2-D, we refer to the monograph (Daubechies, 1992)). For simplicity, we consider 2-D tensor wavelets, that is, we take the tensor product of two 1-D MRAs, with scaling function ϕ, mother wavelet ψ, and diagonal dilation matrix $D = \mathrm{diag}(2, 2)$. Thus we get a 2-D MRA of $L^2(\mathbb{R}^2)$, i.e., an increasing sequence of closed subspaces $\mathbf{V}_j \subset L^2(\mathbb{R}^2)$ with $\bigcap_{j\in\mathbb{Z}} \mathbf{V}_j = \{0\}$ and $\overline{\bigcup_{j\in\mathbb{Z}} \mathbf{V}_j} = L^2(\mathbb{R}^2)$, satisfying the following conditions:

(1) $f(\cdot) \in \mathbf{V}_j \iff f(D\,\cdot) \in \mathbf{V}_{j+1}$,

(2) There exists a function $\Phi \in L^2(\mathbb{R}^2)$ such that the set $\{\Phi(\cdot - \mathbf{k}),\ \mathbf{k} \in \mathbb{Z}^2\}$ is an orthonormal basis (o.n.b.) of $\mathbf{V}_0$.

In terms of the original 1-D MRA, the 2-D scaling function is $\Phi(\mathbf{x}) = \phi(x)\phi(y)$ and for the 2-D MRA it generates, one has

$$\begin{aligned}
\mathbf{V}_{j+1} &= V_{j+1} \otimes V_{j+1} = (V_j \oplus W_j) \otimes (V_j \oplus W_j) \\
&= (V_j \otimes V_j) \oplus [(W_j \otimes V_j) \oplus (V_j \otimes W_j) \oplus (W_j \otimes W_j)] \\
&= \mathbf{V}_j \oplus \mathbf{W}_j.
\end{aligned}$$

Thus $\mathbf{W}_j$ consists of three pieces, with the following orthonormal bases:

$$\{\psi_{j,k_1}(x)\phi_{j,k_2}(y),\ (k_1,k_2)\in\mathbb{Z}^2\} \text{ o.n.b. in } W_j\otimes V_j,$$
$$\{\phi_{j,k_1}(x)\psi_{j,k_2}(y),\ (k_1,k_2)\in\mathbb{Z}^2\} \text{ o.n.b. in } V_j\otimes W_j,$$
$$\{\psi_{j,k_1}(x)\psi_{j,k_2}(y),\ (k_1,k_2)\in\mathbb{Z}^2\} \text{ o.n.b. in } W_j\otimes W_j.$$

This leads us to define three wavelets

$$^h\Psi(x,y)=\phi(x)\psi(y),$$
$$^v\Psi(x,y)=\psi(x)\phi(y),$$
$$^d\Psi(x,y)=\psi(x)\psi(y).$$

Then, $\{^\lambda\Psi_{j,\mathbf{k}},\ \mathbf{k}=(k_1,k_2)\in\mathbb{Z}^2,\ \lambda=h,v,d\}$ is an orthonormal basis for $\mathbf{W}_j$ and $\{^\lambda\Psi_{j,\mathbf{k}},\ j\in\mathbb{Z},\ \mathbf{k}\in\mathbb{Z}^2,\ \lambda=h,v,d\}$ is an orthonormal basis for $\overline{\bigoplus_{j\in\mathbb{Z}}\mathbf{W}_j}=L^2(\mathbb{R}^2)$. Here, for $j\in\mathbb{Z}$, $\mathbf{k}=(k_1,k_2)\in\mathbb{Z}^2$ and for $F\in L^2(\mathbb{R}^2)$, the function $F_{j,\mathbf{k}}$ is defined as

$$F_{j,\mathbf{k}}(x,y)=2^jF(2^jx-k_1,2^jy-k_2).$$

Now we can proceed and lift the MRA to the sphere. To every function $F\in L^2(\mathbb{R}^2)$, one may associate the function $F^s\in L^2(\dot{\mathbb{S}}^2)$ as $F^s=\nu\cdot(F\circ\mathsf{p})$. In particular,

$$F^s_{j,\mathbf{k}}=\nu\cdot(F_{j,\mathbf{k}}\circ\mathsf{p}) \text{ for } j\in\mathbb{Z},\ \mathbf{k}\in\mathbb{Z}^2, \tag{23}$$

and similarly for the spherical functions $\Phi^s_{j,\mathbf{k}}$ and $^\lambda\Psi^s_{j,\mathbf{k}}$, where $\Phi_{j,\mathbf{k}}$,$^\lambda\Psi_{j,\mathbf{k}},\lambda=h,v,d$, are the planar 2-D scaling functions and wavelets, respectively. For $j\in\mathbb{Z}$, we define $\mathcal{V}_j$ as $\mathcal{V}_j:=\{\nu\cdot(F\circ\mathsf{p}),\ F\in\mathbf{V}_j\}$. Then we have:

(1) $\mathcal{V}_j\subset\mathcal{V}_{j+1}$ for $j\in\mathbb{Z}$, and each $\mathcal{V}_j$ is a closed subspace of $L^2(\dot{\mathbb{S}}^2)$;

(2) $\bigcap_{j\in\mathbb{Z}}\mathcal{V}_j=\{0\}$ and $\bigcup_{j\in\mathbb{Z}}\mathcal{V}_j$ is dense in $L^2(\dot{\mathbb{S}}^2)$;

(3) $\{\Phi^s_{0,\mathbf{k}},\ \mathbf{k}\in\mathbb{Z}^2\}$ is an orthonormal basis for $\mathcal{V}_0$.

A sequence $(\mathcal{V}_j)_{j\in\mathbb{Z}}$ of subspaces of $L^2(\dot{\mathbb{S}}^2)$ satisfying (1), (2), (3) constitutes a MRA of $L^2(\dot{\mathbb{S}}^2)$. Define now the wavelet spaces $\mathcal{W}_j$ by $\mathcal{V}_{j+1}=\mathcal{V}_j\oplus\mathcal{W}_j$. Then $\{^\lambda\Psi^s_{j,\mathbf{k}},\ \mathbf{k}\in\mathbb{Z}^2,\ \lambda=h,v,d\}$ is an orthonormal basis for $\mathcal{W}_j$ and $\{^\lambda\Psi^s_{j,\mathbf{k}},\ j\in\mathbb{Z},\ \mathbf{k}\in\mathbb{Z}^2,\ \lambda=h,v,d\}$ is an orthonormal basis for $\overline{\left(\bigoplus_{j\in\mathbb{Z}}\mathcal{W}_j\right)}=L^2(\dot{\mathbb{S}}^2)$. This the orthonormal wavelet basis on $\mathbb{S}^2$.

Thus, an orthonormal 2-D wavelet basis yields an orthonormal spherical wavelet basis. In addition, if Φ has compact support in $\mathbb{R}^2$, then $\Phi^s_{j,\mathbf{k}}$ has local support on $\mathbb{S}^2$ (and $\operatorname{diam}\operatorname{supp}\Phi^s_{j,\mathbf{k}}\to 0$ as $j\to\infty$), and similarly for the respective wavelets. Smooth 2-D wavelets yield smooth spherical wavelets. In particular, Daubechies wavelets yield locally supported and orthonormal wavelets on $\dot{\mathbb{S}}^2$. Thus the same tools as in the planar 2-D case can be used for the decomposition and reconstruction matrices (so that existing toolboxes may be used).

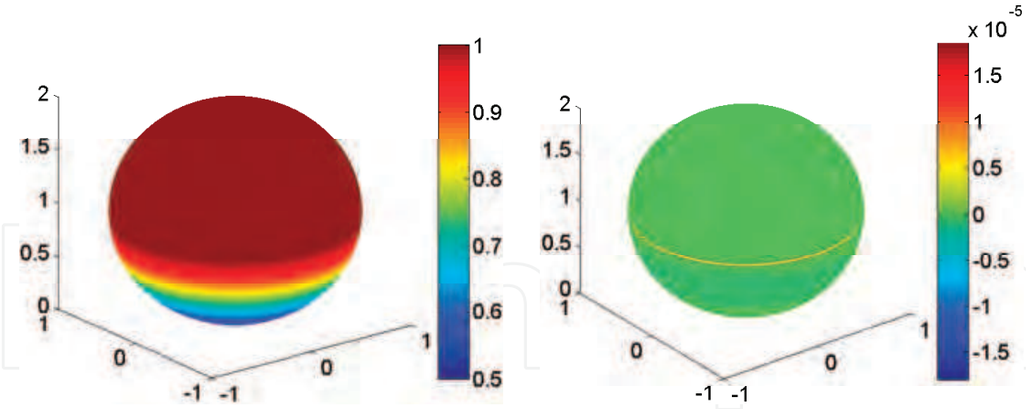

(a) (b)

Fig. 1. (a) The graph of the function $f(\theta, \varphi)$ defined in (24); (b) Its analysis with the spherical wavelet associated to the Daubechies wavelet db3, the familiar 6-coefficient filter.

3.4 An example: Singularity detection

As an application of our construction, we analyse the following zonal function on $\mathbb{S}^2$:

$$f(\theta, \varphi) = \begin{cases} 1, & \theta \leqslant \frac{\pi}{2}, \\ (1 + 3\cos^2\theta)^{-1/2}, & \theta \geqslant \frac{\pi}{2}. \end{cases} \tag{24}$$

The function f and its gradient are continuous, but the second partial derivative with respect to θ has a discontinuity on the equator $\theta = \frac{\pi}{2}$. The function f is shown in Figure 1 (a). Detecting properly such a discontinuity requires a wavelet with three vanishing moments at least, so that, as far as we know, none of the existing constructions of discrete spherical wavelets could detect this discontinuity.

Instead, we consider the discretized spherical CWT with the spherical wavelet $\Psi^s_{H_2}$ associated to the planar wavelet

$$\begin{aligned} \Psi_{H_2}(x, y) &= \Delta^2[e^{-\frac{1}{2}(x^2+y^2)}] \\ &= (x^4 + y^4 + 2x^2y^2 - 8(x^2 + y^2) + 8)e^{-\frac{1}{2}(x^2+y^2)}. \end{aligned} \tag{25}$$

This wavelet has four vanishing moments (again a planar wavelet with less than three vanishing moments could not detect this discontinuity). The analysis is presented in Figure 2. Panels (a), (b), (c) and (d) present the spherical CWT at smaller and smaller scales, $a = 0.08, 0.04, 0.02$ and 0.0165, respectively. From Panels (a)-(c), it appears that the discontinuity along the equator is detected properly, and the precision increases as the scale decreases. However, there is a limit: when the scale a is taken below $a = 0.018$, the singularity is no more detected properly, and the transform is nonzero on the upper hemisphere, whereas the signal is constant there. This is visible on Panel (d), which shows the transform at scale $a = 0.01655$. In fact, the wavelet becomes too narrow and "falls in between" the discretization points, ripples appear in the Southern hemisphere. This effect is described in detail in (Antoine et al., 2002).

On the contrary, the well-known Daubechies wavelet db3 lifted on the sphere by (23) does the job better than the wavelet $\Psi^s_{H_2}$ mentioned above, as one can see in Figure 1, Panel (b). The computational load is smaller and the precision is much better, in the sense that the width of the detected singular curve is narrower.

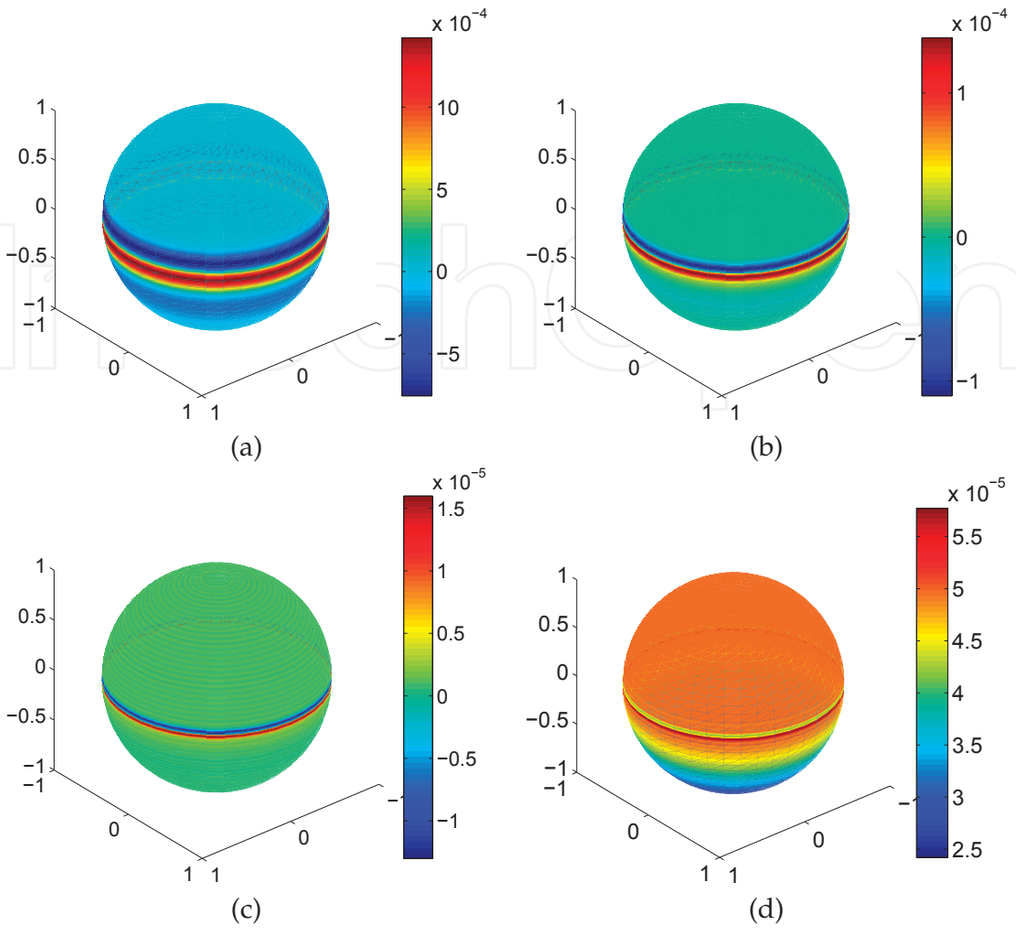

Fig. 2. Analysis of the function $f(\theta, \varphi)$ by the discretized CWT method with the wavelet $\psi^s_{H_2}$, at scales: (a) $a = 0.08$ (b) $a = 0.04$ (c) $a = 0.02$ (d) $a = 0.0165$. The sampling grid is 256×256.

The same tests were performed for the function $f_{\pi/7}$, obtained from f by performing a rotation around the axis Ox with an angle of $\pi/7$. The results are presented in Figure 3. Panel (a) shows the analysis of the function $f_{\pi/7}$ with the discretized CWT method, using the wavelet $\psi^s_{H_2}$, at scale $a = 0.0165$. Panel (b) gives the analysis with the Daubechies wavelet db3 lifted onto the sphere. No appreciable distortion is seen, the detection is good all along the discontinuity circle, and again the precision is better with the lifted Daubechies wavelet. Notice that the computation leading to the figure of Panel (a) was made with a grid finer than that used in Figure 2, so that the detection breaks down at a smaller scale (here below $a = 0.01$).
Of course, this example is still academic, but it is significant. More work is needed, in particular, for estimating the degree of distortion around the pole and applying the method to real life signals.

4. Generalizations

As we have seen up to now in the case of the two-sphere, the main ingredients needed for construction of a wavelet transform on a manifold are harmonic analysis and a proper notion

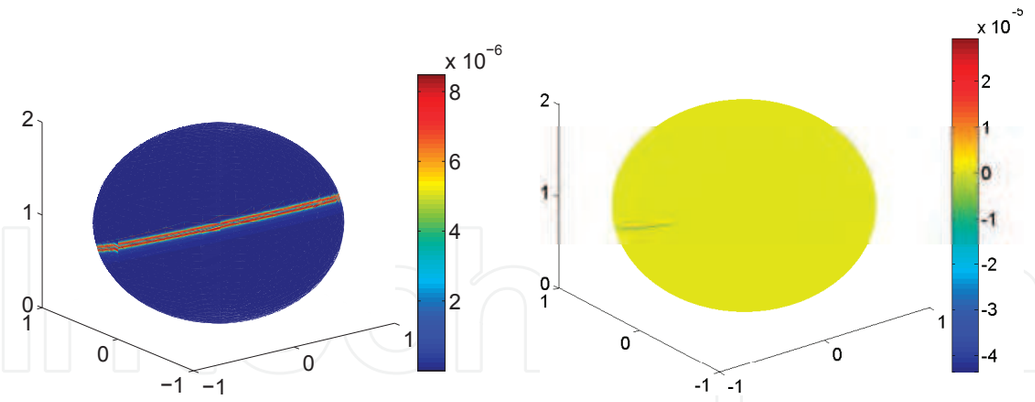

(a) (b)

Fig. 3. (a) Analysis of the function $f_{\pi/7}(\theta,\varphi)$ by the discretized CWT method with the wavelet $\psi^s_{H_2}$, at scale $a = 0.0165$ (the sampling grid here is 512×512); (b) Analysis of the function $f_{\pi/7}(\theta,\varphi)$, with the spherical wavelet associated to db3.

of dilation *on* the manifold. Suitable notions of dilation may be obtained by a group-theoretical approach or by lifting from a fixed plane by some inverse projection.
These generalizations do not have a purely academic interest. Indeed, some data live on manifolds more complicated than the sphere, such as a *two-sheeted hyperboloid* or a *paraboloid*. In optics also, data on such manifolds are essential for the treatment of omnidirectional images, which have numerous applications in navigation, surveillance, visualization, or robotic vision, for instance. In the catadioptric image processing, a sensor overlooks a mirror, whose shape may be spherical, hyperbolic or parabolic. However, instead of projecting the data from that mirror onto a plane, one can process them directly on the mirror, which then suggests to use wavelets on such manifolds (Bogdanova, Bresson, Thiran & Vandergheynst, 2007).

4.1 The two-sheeted hyperboloid $\mathbb{H}^2$

The upper sheet $\mathbb{H}^2_+ = \{\zeta = (\zeta_1,\zeta_2,\zeta_3) \in \mathbb{R}^3,\ \zeta_1^2+\zeta_2^2-\zeta_3^2 = -1,\ \zeta_3 > 0\}$ of the two-sheeted hyperboloid may be treated exactly as the sphere, replacing SO(3) by the isometry group $\mathrm{SO}_o(2,1)$. For dilations, however, a choice has to be made, since there are many possibilities, each type being defined by some projection. Details may be found in (Bogdanova, 2005; Bogdanova, Vandergheynst & Gazeau, 2007). Given an (admissible) hyperbolic wavelet ψ, the hyperbolic CWT of $f \in L^2(\mathbb{H}^2_+)$ with respect to ψ is

$$W_\psi f(g,a) := \langle \psi_{g,a} | f \rangle = \int_{\mathbb{H}^2_+} \overline{\psi_a(g^{-1}\zeta)}\, f(\zeta)\, d\mu(\zeta),\ g \in \mathrm{SO}_o(2,1), a > 0, \tag{26}$$

a formula manifestly analogous to its spherical counterpart (12). As in the spherical case, $\psi_a(\zeta) = \lambda(a,\zeta)\psi(d_{1/a}\zeta)$, with d_a an appropriate dilation, $\lambda(a,\zeta)$ is the corresponding Radon-Nikodym derivative, and μ is the $\mathrm{SO}_o(2,1)$-invariant measure on $\mathbb{H}^2$.
The key for developing the CWT is the possibility of performing harmonic analysis on $\mathbb{H}^2_+$, including a convolution theorem, thanks to the so-called Fourier-Helgason transform. As a consequence, the usual properties hold true, for instance, an exact reconstruction formula. However, no result is known concerning frames that would be obtained by discretization.
On the other hand, it is possible to construct wavelet orthonormal bases on $\mathbb{H}^2_+$ by lifting them from the equatorial plane $\zeta_3 = 0$ by inverse orthographic (i.e., vertical) projection. In this case,

no point has to be avoided, since only one pole is present, but distortions will occur again if one goes sufficiently far away from the tip (pole).

4.2 The paraboloid and other manifolds

Among the three shapes for a catadioptric mirror, the parabolic one is the most common (think of the headlights of a car). And this case brings us back to the topic of Sections 2.2 and 3.3. Indeed it has been shown by Geyer & Daniilidis (2001) that the reconstruction of the orthographic projection from a parabolic mirror can be computed as the inverse stereographic projection from the image plane onto the unit sphere. Thus wavelet frames and wavelet orthogonal bases may be obtained from the corresponding spherical constructions. Alternatively, one may lift planar orthogonal wavelet bases onto the paraboloid directly by inverse orthographic projection, as for the hyperboloid, with the same danger of distortions far away.

For a more general manifold, a local CWT may be designed, using a covering of the manifold by local patches (charts, in the language of differential geometry) and the projection along the normal at the center of each patch (Antoine et al., 2009) (this is also the idea behind needlets (Narcowich et al., 2006b)). One would then get orthogonal wavelet bases in each patch, but there remains the problem of connection of one patch with the next one, using transition functions (the concatenation of all the local bases may also be considered as a dictionary). Notice the same problem of combining local orthogonal wavelet bases has been encountered, and solved, in the wavelet construction based on radial projection from a convex polyhedron (Roşca, 2005), described briefly in Section 3.2(3).

A final example of orthogonal wavelet basis is that of the wavelet transform on graphs (Antoine et al., 2009). A graph is a good model for pairwise relations between objects of a certain collection, such as the nodes of a sensor network or points sampled out of a surface or manifold. Thus a wavelet transform on a graph could be a welcome addition.

A graph is defined as a collection V of vertices or nodes and a collection of edges that connect pairs of vertices. In the present context, one considers finite graphs only, with d nodes. Thus the signals of interest are functions $f : V \to \mathbb{R}$, which can be identified with d-dimensional real vectors $f \in \mathbb{R}^d$. In order to design a wavelet transform on such a graph, one considers the so-called Laplacian matrix, a positive semi-definite $d \times d$ matrix. Its eigenvectors form an orthonormal system that can be used to decompose any signal. Next one defines a dilation by dilating the "Fourier" coefficients — once again the needlet idea. The resulting functions are the wavelets on the graph and they form an orthogonal basis (everything is finite-dimensional). We refer to (Antoine et al., 2009) for further details of the construction.

5. Outcome

We have surveyed a number of techniques for generating orthogonal wavelet bases or wavelet frames on the two-sphere $\mathbb{S}^2$, plus some generalizations. Two approaches have been privileged, both of them based on some notion of inverse projection, namely, (1) the construction of a CWT on $\mathbb{S}^2$ by inverse stereographic projection from a tangent plane, which leads to nontight frames upon discretization; and (2) the construction of orthogonal wavelet bases by lifting in the same way a planar orthogonal basis. Of course, many other methods are available in the literature, especially in the discrete case, and we have mentioned some of them. Clearly many open questions remain, but we want to emphasize that progress in this field is likely to be motivated by physical applications, in particular, astrophysics and optics.

6. References

Antoine, J.-P., Demanet, L., Jacques, L. & Vandergheynst, P. (2002). "Wavelets on the sphere: Implementation and approximations", *Applied Comput. Harmon. Anal.* **13**: 177–200.

Antoine, J.-P., Murenzi, R., Vandergheynst, P. & Ali, S. T. (2004). *Two-dimensional Wavelets and Their Relatives*, Cambridge University Press, Cambridge (UK).

Antoine, J.-P. & Roşca, D. (2008). "The wavelet transform on the two-sphere and related manifolds — A review", *Optical and Digital Image Processing, Proc. SPIE* **7000**: 70000B–1–15.

Antoine, J.-P., Roşca, D. & Vandergheynst, P. (2009). "Wavelet transform on manifolds: Old and new approaches". Preprint.

Antoine, J.-P. & Vandergheynst, P. (1998). "Wavelets on the n-sphere and other manifolds", *J. Math. Phys.* **39**: 3987–4008.

Antoine, J.-P. & Vandergheynst, P. (1999). "Wavelets on the 2-sphere: A group-theoretical approach", *Applied Comput. Harmon. Anal.* **7**: 262–291.

Antoine, J.-P. & Vandergheynst, P. (2007). "Wavelets on the two-sphere and other conic sections", *J. Fourier Anal. Appl.* **13**: 369–386.

Balazs, P., Antoine, J.-P. & Gryboś, A. (2009). "Weighted and controlled frames: Mutual relationship and first numerical properties", *Int. J. Wavelets, Multires. and Inform. Proc.* p. (to appear).

Baldi, P., Kerkyacharian, G., Marinucci, D. & Picard, D. (2008). "high frequency asymptotics for wavelet-based tests for Gaussianity and isotropy on the torus", *J. Multivariate Anal.* **99**(4): 606–636.

Baldi, P., Kerkyacharian, G., Marinucci, D. & Picard, D. (2009). Asymptotics for spherical needlets, *Ann. of Stat.* **37**(3): 1150–1171.

Bogdanova, I. (2005). *Wavelets on non-Euclidean manifolds*, PhD thesis, EPFL, Lausanne, Switzerland.

Bogdanova, I., Bresson, X., Thiran, J.-P. & Vandergheynst, P. (2007). "Scale space analysis and active contours for omnidirectional images", *IEEE Trans. Image Process.* **16**(7): 1888–1901.

Bogdanova, I., Vandergheynst, P., Antoine, J.-P., Jacques, L. & Morvidone, M. (2005). "Stereographic wavelet frames on the sphere", *Appl. Comput. Harmon. Anal.* **26**: 223–252.

Bogdanova, I., Vandergheynst, P. & Gazeau, J.-P. (2007). "Continuous wavelet transform on the hyperboloid", *Applied Comput. Harmon. Anal.* **23**(7): 286–306.

Dahlke, S., Dahmen, W., Schmidt, E. & Weinreich, I. (1995). "Multiresolution analysis and wavelets on S^2 and S^3", *Numer. Funct. Anal. Optim.* **16**: 19–41.

Daubechies, I. (1992). *Ten Lectures on Wavelets*, SIAM, Philadelphia.

Driscoll, J. R. & Healy, D. M. (1994). "Computing Fourier transforms and convolutions on the 2-sphere", *Adv. Appl. Math.* **15**: 202–250.

Freeden, W. & Schreiner, M. (1997). "Orthogonal and non-orthogonal multiresolution analysis, scale discrete and exact fully discrete wavelet transform on the sphere", *Constr. Approx.* **14**: 493–515.

Freeden, W. & Windheuser, U. (1997). "Combined spherical harmonic and wavelet expansion — A future concept in Earth's gravitational determination", *Appl. Comput. Harmon. Anal.* **4**: 1–37.

Geyer, C. & Daniilidis, K. (2001). "Catadioptric projective geometry", *Int. J. Computer Vision* **45**(3): 223–243.

Holschneider, M. (1996). "Continuous wavelet transforms on the sphere", *J. Math. Phys.* **37**: 4156–4165.

Jacques, L. (2004). *"Ondelettes, repères et couronne solaire"*, PhD thesis, Université catholique de Louvain, Louvain-la-Neuve, Belgium.

Marinucci, D., Pietrobon, D., Baldi, A., Baldi, P., Cabella, P., Kerkyacharian, G., Natoli, P., Picard, D. & Vittorio, N. (2008). "spherical needlets for CMB data analysis", *Mon. Not. R. Astron. Soc.* **383**: 539–545.

Narcowich, F. J., Petrushev, P. & Ward, J. D. (2006a). "Decomposition of Besov and Triebel-Lizorkin spaces on the sphere", *J. Funct Anal.* **238**: 530–564.

Narcowich, F. J., Petrushev, P. & Ward, J. D. (2006b). "Localized tight frames on spheres", *SIAM J. Math. Anal.* **38**: 574–594.

Pietrobon, D., Baldi, P. & Marinucci, D. (2006). "Integrated Sachs-Wolfe effect from the cross correlation of WMAP3 year and the NRAO VLA sky survey data: New results and constraints on dark energy", *Phys. Rev. D* **74**: 043524.

Potts, D., Steidl, G. & Tasche, M. (1996). "Kernels of spherical harmonics and spherical frames", *in* F. Fontanella, K. Jetter & P. Laurent (eds), *Advanced Topics in Multivariate Approximation*, World Scientific, Singapore, pp. 287–301.

Roşca, D. (2005). "Locally supported rational spline wavelets on the sphere", *Math. Comput.* **74**(252): 1803–1829.

Roşca, D. (2006). "Piecewise constant wavelets defined on closed surfaces", *J. Comput. Anal. Appl.* **8**(2): 121–132.

Roşca, D. (2007a). "Wavelet bases on the sphere obtained by radial projection", *J. Fourier Anal. Appl.* **13**(4): 421–434.

Roşca, D. (2007b). Weighted Haar wavelets on the sphere, *Int. J. Wavelets, Multires. and Inform. Proc.* **5**(3): 501–511.

Roşca, D. (2009). "On a norm equivalence on $L^2(S^2)$", *Results Math.* . (53(3-4):399-405).

Roşca, D. & Antoine, J.-P. (2008). "Constructing orthogonal wavelet bases on the sphere", *in* J.-P. Thiran (ed.), *Proc. 16th European Signal Processing Conference (EUSIPCO2008)*, EPFL, Lausanne, Switzerland. Paper # 1569102372.

Roşca, D. & Antoine, J.-P. (2009). "Locally supported orthogonal wavelet bases on the sphere via stereographic projection". Math. Probl. Eng vol. 2009, art ID 124904 (14 pages).

Weinreich, I. (2001). "A construction of C^1-wavelets on the two-dimensional sphere", *Applied Comput. Harmon. Anal.* **10**: 1–26.

Wiaux, Y., Jacques, L. & Vandergheynst, P. (2005). "Correspondence principle between spherical and Euclidean wavelets", *Astrophys. J.* **632**: 15–28.

Wiaux, Y., McEwen, J. D., Vandergheynst, P. & Blanc, O. (2008). "Exact reconstruction with directional wavelets on the sphere", *Mon. Not. R. Astron. Soc.* **388**: 770.

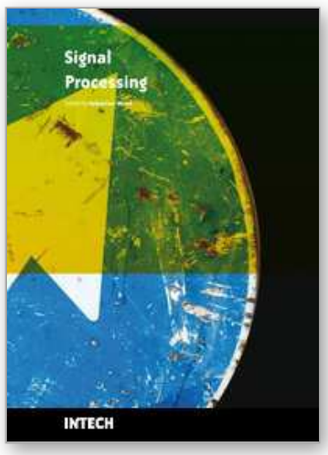

Signal Processing

Edited by Sebastian Miron

ISBN 978-953-7619-91-6
Hard cover, 528 pages
Publisher InTech
Published online 01, March, 2010
Published in print edition March, 2010

This book intends to provide highlights of the current research in signal processing area and to offer a snapshot of the recent advances in this field. This work is mainly destined to researchers in the signal processing related areas but it is also accessible to anyone with a scientific background desiring to have an up-to-date overview of this domain. The twenty-five chapters present methodological advances and recent applications of signal processing algorithms in various domains as telecommunications, array processing, biology, cryptography, image and speech processing. The methodologies illustrated in this book, such as sparse signal recovery, are hot topics in the signal processing community at this moment. The editor would like to thank all the authors for their excellent contributions in different areas of signal processing and hopes that this book will be of valuable help to the readers.

InTech Europe
University Campus STeP Ri
Slavka Krautzeka 83/A
51000 Rijeka, Croatia
Phone: +385 (51) 770 447
Fax: +385 (51) 686 166
www.intechopen.com

InTech China
Unit 405, Office Block, Hotel Equatorial Shanghai
No.65, Yan An Road (West), Shanghai, 200040, China
中国上海市延安西路65号上海国际贵都大饭店办公楼405单元
Phone: +86-21-62489820
Fax: +86-21-62489821

IntechOpen